Fast Finite-Difference Time-Domain Analysis of Resonators Using Digital Filtering and Spectrum Estimation Techniques

Zhiqiang Bi, *Student Member, IEEE,* Ying Shen, Keli Wu, *Member, IEEE,* and John Litva, *Member, IEEE*

Abstract—**In this paper we discuss the use of digital filtering and spectrum estimation techniques for improving the efficiency of the FD-TD algorithm in solving eigenvalue problems. The great improvement of the efficiency of the method is demonstrated by means of both numerical and measurement results. In addition, several improvements to the present FD-TD method for eigenvalue analysis are presented. These include the analysis of open dielectric resonators and the extraction of the resonant frequencies from the FD-TD results. The result for the open dielectric resonator analysis is validated using measured data.**

I. Introduction

THE OPTIMIZATION of the performance of resonators in microwave circuits requires accurate and efficient methods for calculating the resonant frequencies and the spatial distributions of the field. Various methods have been developed to study the resonant frequencies of resonant structures. Most of them, such as; the mode matching method, integral equation method, and finite element method, are carried out in the frequency domain [1].

The finite-difference time-domain (FD-TD) method has been widely used for solving electromagnetic problems. Resently, it has been used to solve eigenvalue problems associated with resonator structures [2], [3] and to calculate critical parameters for complex microstrip antennas [4], [5]. All of these results have shown the FD-TD method to be a very powerful tool for eigenvalue analysis, primarily because of two desirable attributes. First, it can be applied to problems exhibiting a complex structure which may be very difficult to solve using other analytical or numerical methods. Second, only one computation is required to get the frequency domain results over a large frequency spectrum. However, this method has one significant drawback, which is that it requires a very long computation time for extracting the resonant frequencies from the FD-TD results; for example, in the case of the problem discussed in [2], the time iteration N has to be as large as $N = 2^{16}$.

The main purpose of this paper is to introduce the use of digital filtering and modern spectrum estimation techniques with the FD-TD method, as a means for overcoming above limitation. By using numerical results, it will be shown that modern spectrum estimation techniques can reduce the time taken to solve a problem, such as that discussed in [2], by one order of magnitude, without any loss of accuracy in calculating the resonant frequencies. It follows from this example, that, in general, the FD-TD computational time for these types of problems can be reduced by one order of magnitude. In addition, several other improvements to the method used in [2] are presented in this paper. These include the ability to analyze open dielectric resonators, the technique for extracting the resonator frequencies, as well as the calculation of the field distribution, from the FD-TD results.

Manuscript received October 7, 1991; revised February 5, 1992.

The authors are with the Communications Research Laboratory, McMaster University, 1280 Main Street West, Hamilton, ON L85 4K1, Canada.

IEEE Log Number 9200847.

II. FD-TD Method for Resonator Analysis

For ease of description, the method is described by referring to the generalized cylindrical shaped dielectric resonator (DR) in Fig. 1. This structure is rotationally symmetric. Since $TE_{01\delta}$ modes are the most commonly used for DR applications, only the TE_0 modes are discussed. The relevant form of Maxwell's equations are

$$\frac{\partial}{\partial t}(\epsilon E_\theta) = \frac{\partial H_r}{\partial z} - \frac{\partial H_z}{\partial r} \tag{1}$$

$$\frac{\partial}{\partial t}(\mu H_r) = \frac{\partial E_\theta}{\partial z} \tag{2}$$

$$\frac{\partial}{\partial t}(\mu H_z) = -\frac{1}{r}\frac{\partial (rE_\theta)}{\partial r}. \tag{3}$$

Using a central difference scheme similar to that used by Yee [6], the above equations can be discretized as

$$\begin{aligned} E_\theta^{n+(1/2)}(i,j) &= E_\theta^{n-(1/2)}(i,j) + \frac{\Delta t}{\Delta z \epsilon}\left[H_r^n\left(i, j+\frac{1}{2}\right) - H_r^n\left(i, j-\frac{1}{2}\right)\right] \\ &\quad - \frac{\Delta t}{\Delta r \epsilon}\left[H_z^n\left(i+\frac{1}{2}, j\right) - H_z^n\left(i-\frac{1}{2}, j\right)\right] \end{aligned} \tag{4}$$

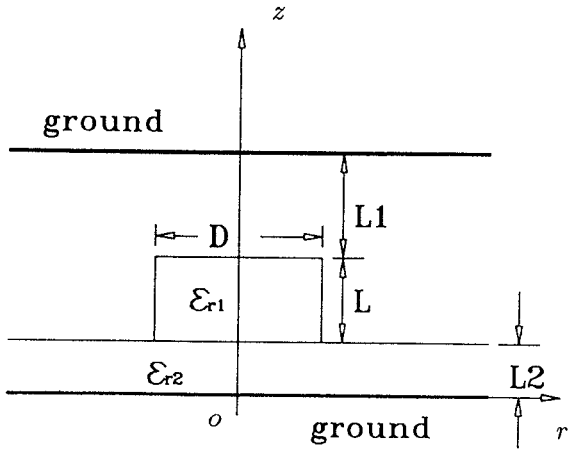

Fig. 1. A generalized cylindrical shape dielectric resonator.

$$H_r^{n+1}\left(i, j-\frac{1}{2}\right) = H_r^n\left(i, j-\frac{1}{2}\right) + \frac{\Delta t}{\mu\,\Delta z} \cdot \left[E_\theta^{n+(1/2)}(i, j) - E_\theta^{n+(1/2)}(i, j-1)\right] \quad (5)$$

$$H_z^{n+1}\left(i+\frac{1}{2}, j\right) = H_z^n\left(i+\frac{1}{2}, j\right) - \frac{\Delta t}{\mu\,\Delta r r_{i+(1/2)}} \cdot \left[r_{i+1}E_\theta^{n+(1/2)}(i+1, j) - r_i E_\theta^{n+(1/2)}(i, j)\right] \quad (6)$$

where i and j are space index and n is the time index.

The computation domain diagram is shown in Fig. 2. The tangential electric field components are located at the interfaces between different materials and on the outer boundaries of the computation domain. The fields at the interfaces between different materials can still be calculated using (4), if it is remembered that average of the two dielectric constants, $(\epsilon_1 + \epsilon_2)/2$, has to be used in place of ϵ in the equation. Using a derivation similar to that used in [7], it can be proved that, for the fields at an interface between three media, the effective dielectric constant becomes $(\epsilon_1 + \epsilon_2 + \epsilon_3)/3$, and for four media, it becomes $(\epsilon_1 + \epsilon_2 + \epsilon_3 + \epsilon_4)/4$.

The previous analyses given in [2], [3] are limited to a consideration of a closed resonator, where the tangential electric fields on the outer boundaries are forced to be zero. Actually, by using the well developed absorbing boundary condition (ABC) in conjunction with the FD-TD method [8], the method can be extended so that it can deal with the open structure problem. In this paper, Mur's first-order boundary condition [9] is used:

$$\left(\frac{\partial}{\partial z} + \frac{1}{v_p}\frac{\partial}{\partial t}\right) E = 0 \quad (7)$$

where E represents the tangential electric field component relative to the boundary wall and v_p represents the phase

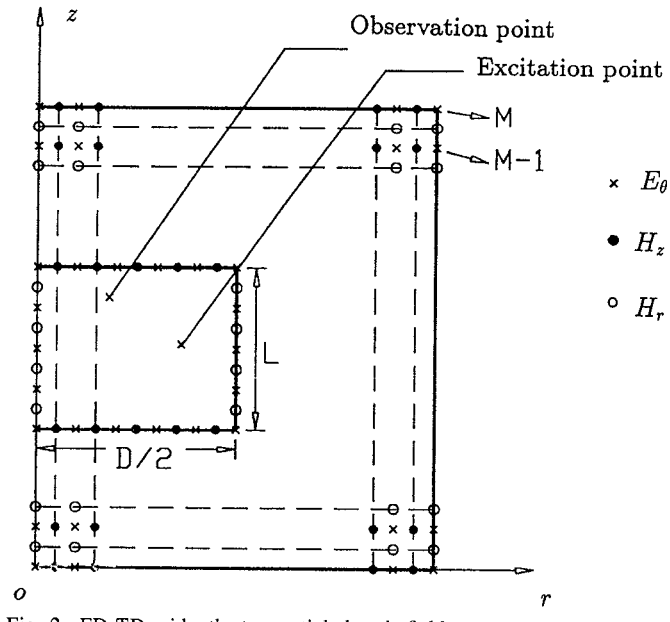

Fig. 2. FD-TD grids, the tangential electric field components are arranged on the interface of different materials and on the outer boundaries of the computation domain.

velocity of the field. This equation is easily discretized using only field components on and just inside the mesh wall, yielding the difference equation

$$E_M^n = E_{M-1}^{n-1} + \frac{\Delta z - v_p\,\Delta t}{\Delta z + v_p\,\Delta t}\left(E_M^{n-1} - E_{M-1}^n\right) \quad (8)$$

where E_M represents the tangential electric field component on the boundary and E_{M-1} represents the tangential electric field component a distance of one node inside the boundary. The other absorbing boundary conditions [8] can be applied to improve the accuracy. But, according to our experience, the first order ABC has sufficient accuracy to deal with high dielectric constant resonators.

To start the computation, the initial electric and magnetic fields are set to zero throughout the grid, except at one selected point. Here the electric field is set to 1. This unit impulse source will excite a large number of modes. Using the above algorithm, Fig. 3(a) gives the computed electric field in the time domain at the point of observation. The resonant frequencies can be obtained by taking the Fourier transform of the computed time domain response. The field distributions for any particular frequency can be obtained by performing Fourier transform at each point in the computation domain at that frequency. With the objective of getting more accurate estimates of the resonant frequency and field distribution than that have been obtained in the past, the following procedure is put forward.

The procedure to be followed is based on the signal analysis of the time domain results obtained using the FD-TD method. In this section, it is assumed that the sequence length of the FD-TD result $\{x(n)\}$ is very long, where $x(n)$ is one of the field components. At an earlier stage of the FD-TD method, the fast Fourier Transform (FFT) algorithm is used to calculate the discrete Fourier

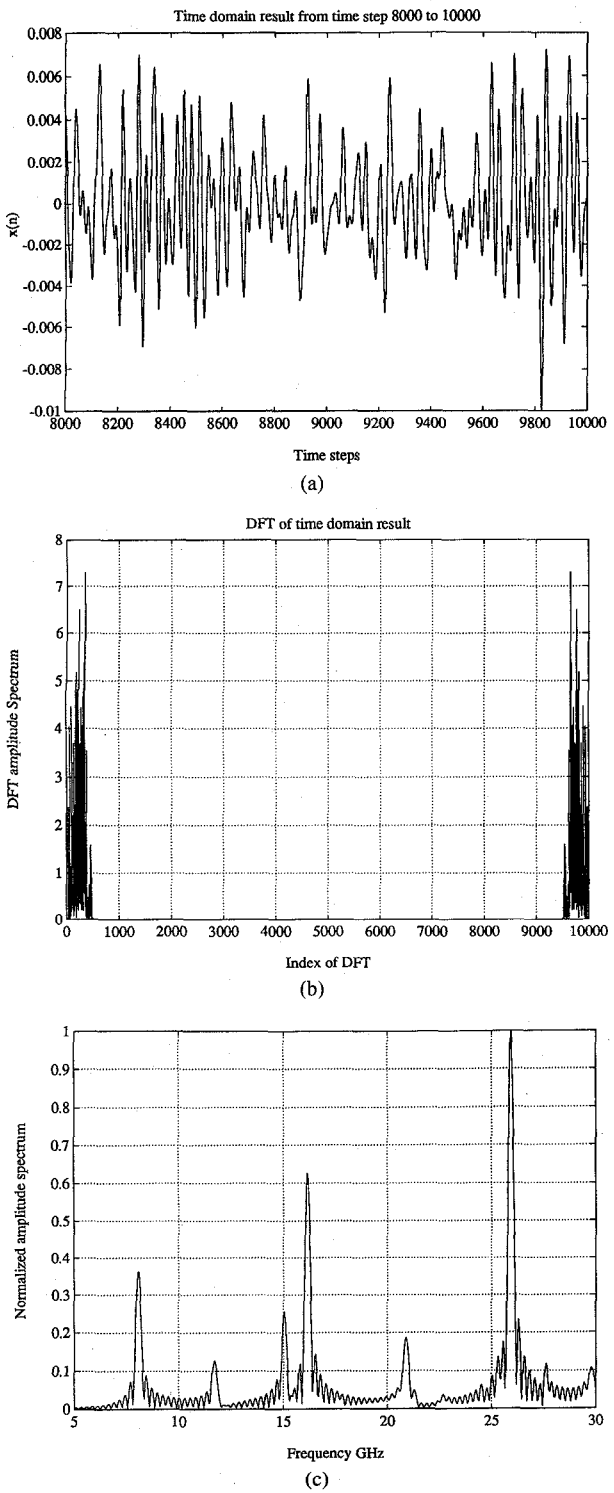

Fig. 3. (a) Time domain result directly obtained from the FD-TD algorithm. (b) Its corresponding DFT spectrum. (c) Normalized amplitude spectrum of Fourier transform of long sequence and desampled shorter sequence.

transform (DFT) of $\{x(n)\}$ to get the spectrum, $X(f)$, of $x(t)$, where $x(n) = x(t)|_{t=n\Delta t}$ and Δt is the time step used in the FD-TD algorithm. For some applications [10], this method is not very efficient and it does not have sufficient accuracy. This is because the $N/2$ values of DFT are uniformly distributed over a very large frequency bandwidth, extending from 0 to $f_s/2$ Hz, where $f_s = 1/\Delta t$ is the sampling frequency, and because the frequency resolution, which is given by

$$\Delta f = \frac{1}{N \cdot \Delta t}, \tag{9}$$

where N is the length of the sequence $\{x(n)\}$, is too coarse to accurately determine resonant frequencies. In practice, only the lower part of the band is of interest. One method that has been suggested here is to do the numerical integration of Fourier Transform of $x(t)$ directly in the interested frequency band

$$\begin{aligned} X(f) &= \int_0^{\infty} x(t) \exp(-j2\pi ft)\, dt \\ &\approx \int_0^{N\Delta t} x(t) \exp(-j2\pi ft)\, dt \\ &\approx \sum_{n=0}^{N-1} x(n) \exp(-j2\pi fn\,\Delta t)\,\Delta t. \end{aligned} \tag{10}$$

The advantage of this method is that it removes ambiguities sometimes encountered with the discrete Fourier Transform, due to narrowband signal components with center frequencies that lie in the gaps between the $N/2$ frequency points evaluated with the DFT. It will be shown in the following that, when FD-TD method is used for resonator analysis, the time domain results are signals which consist of many narrowband signal components. The accuracy of calculating the spectral peaks, i.e., the field distribution, is also enhanced by using (10).

The efficiency of calculating (10) can be greatly improved by using the following method. Instead of using the original sequence $\{x(n)\}$ obtained using the FD-TD result, a new sequence $\{x_1(n)\}$ is used in (10), which is obtained by desampling the $\{x(n)\}$ at a certain rate. The desampling rate is determined by the ratio of the half sampling frequency $f_s/2$ to the maximum frequency $f_{\max}$ of the long sequence $\{x(n)\}$. Because $\{x_1(n)\}$ is much shorter than the original sequence $\{x(n)\}$, the time required to analyze the new time domain sequence can be greatly reduced, with no reduction in the accuracy of the result. The theory which supports this treatment is Nyquist sampling theorem [11].

In order to illustrate the method clearly, let us refer to the dielectric resonator problem in Fig. 1. In Fig. 3(a) is given the time domain results for the observation point shown in Fig. 2. This result was obtained using the FD-TD method. The DFT spectrum corresponding to this result is given in Fig. 3(b). The parameters used in the calculation are

Dimension: $D = 6.26$ mm, $L = 4.22$ mm,
$L_1/L = 0.943$ mm, $L_2/L = 0.166$ mm
$\epsilon_{r1} = 36.2$, $\epsilon_{r2} = 9.5$
Mesh dimensions in dielectric region: 24 $\Delta z \times 18\ \Delta r$
$\Delta z = 0.17583$ mm, $\Delta r = 0.175824$ mm
$\Delta t = 0.65(\Delta z + \Delta r)/(2c)$, c is the speed of light in free space

According to the Nyquist theorem and from the spectrum in Fig. 3(b), it follows that the original sequence $\{x(n)\}$ is a much over-sampled time domain signal, and that a new sequence $\{x_1(n)\}$ can be obtained by using a desampling rate of about 10. In Fig. 3(c), the solid line gives the result obtained by appling (10) to the long sequence, and the dashed line gives the result obtained by applying (10) to the decimated sequence $\{x_1(n)\}$. The two results are exactly the same and therefore overlap in Fig. 3(c).

After getting the much shorter sequence $\{x_1(n)\}$, the numerical integration of (10) can also be calculated using a FFT program in the following manner. First, pad zero values to the decimated sequence $\{x_1(n)\}$, then apply FFT to the padded sequence. The number of padded zeros are determined by the frequency resolution requirement.

Another phenomena that needs some explanation is why the results, $\{x(n)\}$, obtained from the FD-TD analysis, which can be thought as a unit impulse response, only contain components at the lower end of the frequency spectrum. The answer lies in the dispersion that is introduced to the results by the FD-TD algorithm itself [12], [13]. Another simpler explanation to this phenomena is that the wavelength of the waves which can freely propagate in the FD-TD grid should be at least two grid spaces. Otherwise, the grids are too coarse to describe (support) wave movement, thereby preventing waves from propagating on the FD-TD grid. The corresponding cutoff frequency is the maximum frequency of the FD-TD time domain result, which is equal to about $f_{\max} = v/(2\ \Delta h)$, where v is the speed of light in the dielectric materials and Δh is the space step (where a uniform grid is assumed). For dielectric resonator analysis, because most of the energy is centered in the material which has the largest dielectric constant, the velocity $v = c/\sqrt{\epsilon_{\max}}$ should be used to determine the maximum frequency of the time domain result of FD-TD method, where c is the velocity of light in free space. Once the maximum frequency $f_{\max}$ is known, the desampling rate can be determined.

III. Use of Digital Filtering and Modern Spectrum Estimation Techniques with FD-TD Method

The objective of this section is, based on a much shorter sequence $\{x_2(n)\}$ obtained directly from the output FD-TD algorithm, to use digital filtering and modern spectrum estimation techniques to extract the resonant frequencies of the dielectric resonator. Suppose $\{x_2(n)\}$ is the sequence consisting of the first two thousand data points in $\{x(n)\}$. The DFT spectrum of $\{x_2(n)\}$ is shown in Fig. 4(a). After desampling $\{x_2(n)\}$, using a desampling rate of $(f_s/2)/f_{\max}$, which is about 10, we get a sequence $\{x_3(n)\}$ whose DFT spectrum is shown in Fig. 4(b). Because we are interested in the lower frequency band, we further process the signal $\{x_3(n)\}$ by using a decimating filter to get $\{x_4(n)\}$, whose DFT spectrum is shown in Fig. 4(c). In applying the decimating filter [14], we first pass the data through a low-pass digital filter, then, according to the maximum frequency of the filtered output, we desample the filtered output to get the final output signal. In order to improve the accuracy of estimating the resonant frequencies of the first few modes, we further process $\{x_4(n)\}$ with a low-pass filter and get $\{y(n)\}$, whose DFT spectrum is shown in Fig. 4(d). In all cases, ninth order Butterworth filters are used to carry out the filtering. In the filtering process, the data are filtered in both the forward and backward directions, thereby eliminating all phase distortion and minimizing filter startup transients [15]. In the next phase of the work we carry out a search for a good high resolution spectrum estimator, with which to extract the resonant frequencies from the data $\{y(n)\}$.

From the behavior of the spectrum of $\{x(n)\}$, based on the results given in Fig. 3c, it seems reasonable to assume that $\{y(n)\}$ is composed of sinusoidal components. One of the best kinds of methods for estimating the frequencies of sinusoidal components is the multiple signal classification (MUSIC) method [16]–[18]. This method belongs to the eigendecomposition-based class of super-resolution spectrum estimation methods. The term "super-resolution" refers to the fact that this class of methods have the ability to surpass the limiting behavior of classical Fourier-based methods. There are a number of reasons for our choosing the MUSIC algorithm from amongst this class of methods. These are: (i) it is easy to implement, (ii) it provides good performance, (iii) it is used as a bench mark in the field of signal processing, and (iv) it provides a good introduction to modern spectrum estimation.

The general aim of eigendecomposition-based methods is to exploit the eigenvalue decomposition of the correlation matrix of a signal consisting of p uncorrelated complex sinusoids and additive complex white noise. The signal is:

$$y(n) = \sum_{i=1}^{p} A_i \exp\left(j2\pi f_i n\ \Delta t + \theta_i\right) + w(n) \quad (11)$$

where the amplitudes $\{A_i\}$ are real-valued positive constants, the initial phases $\{\theta_i\}$ are independent random variables distributed uniformly on $[0, 2\pi]$, and the frequencies $\{f_i\}$ are distinct, Δt is the sample interval of the signal $\{y(n)\}$ and $\{w(n)\}$ is complex white noise with zero mean and variance σ^2. Although here we discuss frequency estimation for p complex sinusoids in complex white noise, the same methods generally apply to real sinusoids in real white noise if p is chosen to be twice the number of real sinusoids. The autocorrelation function of the above signal is

$$\begin{aligned} r(k) &= E[y(n)y^*(n-k)] \\ &= \sum_{i=1}^{p} A_i^2 \exp\left(j2\pi f_i k\ \Delta t\right) + \sigma^2\,\delta(k) \end{aligned} \quad (12)$$

where E denotes the expectation operator and * denotes complex conjugate. The corresponding $(M+1) \times (M+$

1) ensemble-averaged autocorrelation matrix

$$\boldsymbol{R} = \begin{bmatrix} r(0) & r(1) & \cdots & r(M) \\ r(-1) & r(0) & \cdots & r(M-1) \\ \cdot & \cdot & \cdots & \cdot \\ \cdot & \cdot & \cdots & \cdot \\ \cdot & \cdot & \cdots & \cdot \\ r(-M) & r(-M+1) & \cdots & r(0) \end{bmatrix} \tag{13}$$

for $M > p$ is

$$\boldsymbol{R} = \boldsymbol{S}\boldsymbol{D}\boldsymbol{S}^H + \sigma^2\boldsymbol{I} \tag{14}$$

where $\boldsymbol{I}$ is the $(M+1) \times (M+1)$ identity matrix, the rectangular matrix $\boldsymbol{S}$ is the $(M+1) \times p$ sinusoidal signal matrix defined as

$$\boldsymbol{S} = [s_1, s_2, \cdots s_p] = \begin{bmatrix} 1 & 1 & \cdots & 1 \\ \exp(-j2\pi f_1 \Delta t) & \exp(-j2\pi f_2 \Delta t) & \cdots & \exp(-j2\pi f_p \Delta t) \\ \exp(-j2\pi f_1 2\Delta t) & \exp(-j2\pi f_2 2\Delta t) & \cdots & \exp(-j2\pi f_p 2\Delta t) \\ \cdot & \cdot & \cdots & \cdot \\ \cdot & \cdot & \cdots & \cdot \\ \cdot & \cdot & \cdots & \cdot \\ \exp(-j2\pi f_1 M\Delta t) & \exp(-j2\pi f_2 M\Delta t) & \cdots & \exp(-j2\pi f_p M\Delta t) \end{bmatrix}, \tag{15}$$

$\boldsymbol{D}$ is the $p \times p$ correlation matrix of the sinusoids, and ^{H} denotes conjugate transpose. Note that the lth column of the matrix $\boldsymbol{S}$, namely s_l is a signal vector of dimension $(M+1)$ carrying the frequency information of the lth complex sinusoid. Let $\lambda_1 \geq \lambda_2 \cdots \geq \lambda_{M+1}$ denote the eigenvalues of the correlation matrix $\boldsymbol{R}$, and $v_1 \geq v_2 \cdots \geq v_{M+1}$ denote the eigenvalues of $\boldsymbol{S}\boldsymbol{D}\boldsymbol{S}^H$, respectively. Since $\boldsymbol{S}$ is a full rank matrix and $\boldsymbol{D}$ is positive definite, it follows [16] that

$$\lambda_i = \begin{cases} v_i + \sigma^2, & i = 1, \cdots, p \\ \sigma^2, & i = p+1, \cdots, M+1 \end{cases} \tag{16}$$

Let $\boldsymbol{v}_1, \boldsymbol{v}_2, \cdots, \boldsymbol{v}_{M+1}$ denote the eigenvectors of the correlation matrix $\boldsymbol{R}$. All the $(M+1-p)$ eigenvectors associated with the smallest eigenvalues of $\boldsymbol{R}$ satisfy the relation

$$\boldsymbol{R}\boldsymbol{v}_i = \sigma^2\boldsymbol{v}_i, \quad i = p+1, \cdots, M+1 \tag{17}$$

or, equivalently,

$$(\boldsymbol{R} - \sigma^2\boldsymbol{I})\boldsymbol{v}_i = \boldsymbol{0}, \quad i = p+1, \cdots, M+1 \tag{18}$$

Using (14), the above equation can be rewritten as

$$\boldsymbol{S}\boldsymbol{D}\boldsymbol{S}^H\boldsymbol{v}_i = \boldsymbol{0}, \quad i = p+1, \cdots, M+1 \tag{19}$$

It readily follows that

$$\boldsymbol{S}^H\boldsymbol{v}_i = \boldsymbol{0}, \quad i = p+1, \cdots, M+1 \tag{20}$$

or more explicitly

$$s_l^H\boldsymbol{v}_i = 0, \quad i = p+1, \cdots, M+1, \quad l = 1, 2, \cdots, p \tag{21}$$

where the vector s_l constitutes the lth column of matrix $\boldsymbol{S}$.

A fundamental property of the eigenvectors of a correlation matrix is that they are orthogonal to each other. Hence, the eigenvectors $\boldsymbol{v}_1, \cdots, \boldsymbol{v}_p$ span a subspace that is the orthogonal complement of the space spanned by the eigenvectors $\boldsymbol{v}_{p+1}, \cdots, \boldsymbol{v}_{M+1}$. Accordingly, it follows from (21) that

$$\text{span}\{s_1, \cdots, s_p\} = \text{span}\{\boldsymbol{v}_1, \cdots, \boldsymbol{v}_p\} \tag{22}$$

The span $\{s_1, \cdots, s_p\}$ refers to a subspace that is defined by the set of all linear combinations of the vectors $s_1, \cdots, s_p$. The span $\{\boldsymbol{v}_1, \cdots, \boldsymbol{v}_p\}$ is similarly defined.

Based on the above discussions, we can conclude the following important property of the eigenvalue decomposition of the $(M+1) \times (M+1)$ correlation matrix $\boldsymbol{R}$ of the signal defined in (11), which is

> The space spanned by the eigenvectors of $\boldsymbol{R}$ consists of two disjoint subspaces. One called signal subspace, is spanned by the eigenvectors associated with the p largest eigenvalues of $\boldsymbol{R}$. The second subspace called the noise subspace, is spanned by the eigenvectors associated with the $(M+1-p)$ smallest eigenvalues of $\boldsymbol{R}$. These two subspace are the orthogonal complement of each other and they satisfy the (21) and (22).

Various eigendecomposition-based methods exploit the above property, i.e. the existence of two subspaces in different ways. The approach used in the MUSIC algorithm is to estimate the frequencies of the complex sinusoids by searching for those sinusoidal signal vectors s_l that are orthogonal to the noise subspace. This follows from (21).

In practice, the implementation of all these different methods uses the sample estimation of the ensemble-averaged correlation matrix $\boldsymbol{R}$. One of the best estimations [17] for $\boldsymbol{R}$ is

$$\hat{\boldsymbol{R}} = \frac{1}{2(K-M)}\boldsymbol{\Phi} \tag{23}$$

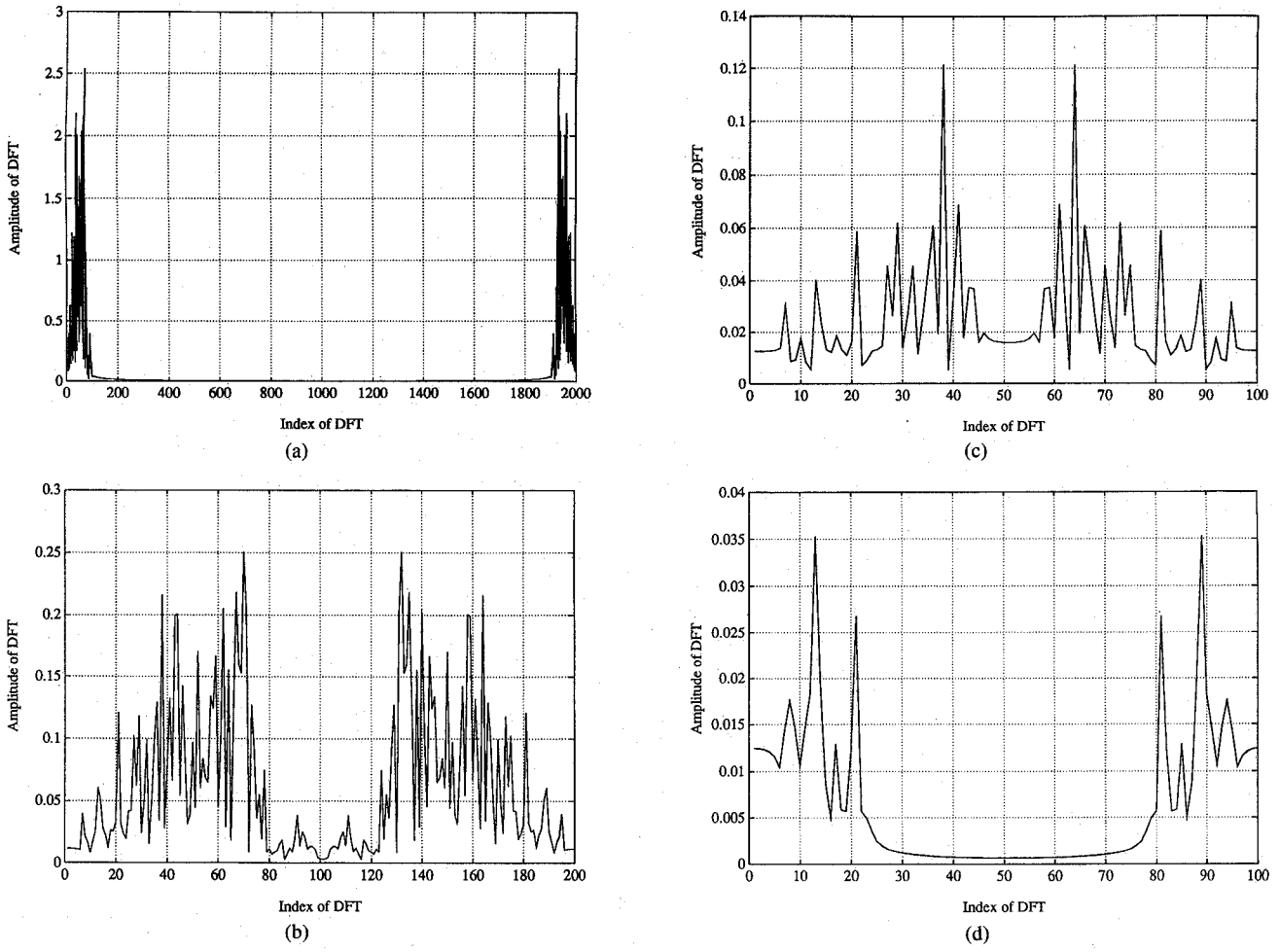

Fig. 4. Digital filtering processing of the FD-TD time domain result. (a)–(d) DFT spectrums.

where K is the sequence length of $\{y(n)\}$ and Φ is

$$\Phi = A^H A \tag{24}$$

where A^H is defined as

$$A^H = \begin{bmatrix} y(M) & \cdots & y(K-1) & y^*(0) & \cdots & y^*(K-M+1) \\ y(M-1) & \cdots & y(K-2) & y^*(1) & \cdots & y^*(K-M+2) \\ \cdot & \cdots & & \cdot & \cdots & \\ \cdot & \cdots & & \cdot & \cdots & \\ \cdot & \cdots & & \cdot & \cdots & \\ y(0) & \cdots & y(K-M+1) & y^*(M) & \cdots & y^*(K-1) \end{bmatrix}. \tag{25}$$

Let $\hat{v}_1, \hat{v}_2, \cdots, \hat{v}^{M+1}$ denote the eigenvectors of the estimate $\hat{R}$. Owing to the presence of uncertainties in the eigenvector estimates, $\hat{v}_1, \hat{v}_2, \cdots, \hat{v}^{M+1}$, arising from the limited number of samples that are available in practice for deriving the estimate, $\hat{R}$, the orthogonality relations of (21) no longer strictly hold. Accordingly, the MUSIC algorithm bases its estimates of the frequencies of the complex sinusoids in the data vector on locating the peaks in the expression

$$\hat{Y}_{\text{MUSIC}}(f) = \frac{1}{\sum_{i=p+1}^{M+1} |s^H \hat{v}_i|^2} \tag{26}$$

where the frequency scanning vector $s(f)$ is defined by

$$s(f) = [1, \exp(-j2\pi f \Delta t), \cdots, \exp(-j2\pi f M \Delta t)]^T \tag{27}$$

where ^{T} denotes transpose. It should be pointed out that MUSIC spectrum $\hat{Y}_{\text{MUSIC}}(f)$ is not a true power spectrum because it does not preserve the power of the signal nor

can the autocorrelation sequence be recovered by Fourier Transforming the frequency estimator.

The MUSIC algorithm can be summarized below

1. Set up data matrix $\boldsymbol{A}$ using (25) and calculate the estimate $\hat{\boldsymbol{R}}$ of the $(M + 1) \times (M + 1)$ correlation matrix using (23). Computer the the eigenvalues and eigenvectors of $\hat{\boldsymbol{R}}$.
2. Given that there are p complex sinusoids in the input signal, with $p \leq M$, classify the eigenvalues into two groups. One consisting of the p largest eigenvalues and the other consisting of the $(M + 1 - p)$ smallest eigenvalues. The first group spans the sample signal subspace, the second group spans the sample noise subspace.
3. Use the eigenvectors associated with the second group to calculate the MUSIC spectrum (26). Determine the frequencies of the complex sinusoids by locating the spectral peaks of $\hat{Y}_{\text{MUSIC}}(f)$.
4. In place of procedure 3, the frequencies can also be determined by using root-MUSIC [19].

IV. Numerical Results

Using the above MUSIC algorithm, the signal $\{y(n)\}$ which was obtained after filtering processing in the last section is analyzed. The result is shown in Fig. 5. The dashed line was obtained by applying a Fourier transform (10) to a very long FD-TD sequence, corresponding to 20 000 time iterations in the FD-TD algorithm. The dotted curve gives the result from Fourier processing (10) of the first two thousand points in the former sequence. This shortened sequence corresponds to 2000 time iterations in the FD-TD algorithm. From this curve we see that, for short data records, the resonant frequencies cannot be accurately estimated using the Fourier transform. Biases occur in the locations of the first and fourth resonant frequencies and the second and third resonant frequencies are missing altogether. The solid line gives the result of application of digital filtering and the MUSIC spectral estimation technique to the shorter data. In the MUSIC algorithm, the data length of $\{y(n)\}$, K, was equal to 100, the order of the correlation matrix $M + 1$, was determined by the relation $M = 2K/3$. The accuracy of the method increases with increasing M [16]. However, $M + 1$ should not be larger than the number of data points. The choice for the order of the signal subspace, p, is based on the eigenvalue spectrum of $\hat{\boldsymbol{R}}$. For our example, p was equal to 21. When p was changed from 21 to a higher value, we still got accurate frequency estimates. This suggests that the method is robust. Comparing the solid and dashed lines, it is seen that the same order or accuracy is obtained in the resonant frequency estimation by applying signal processing and spectral estimation to a short data set as that obtained by applying a Fourier transform to a much longer data set.

A semi-open dielectric resonator coupled to a microstrip substrate (Fig. 6) is also studied. The parameters used for this analysis are

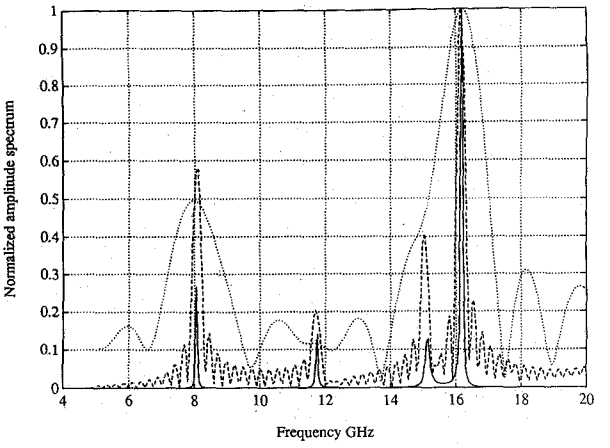

(a)

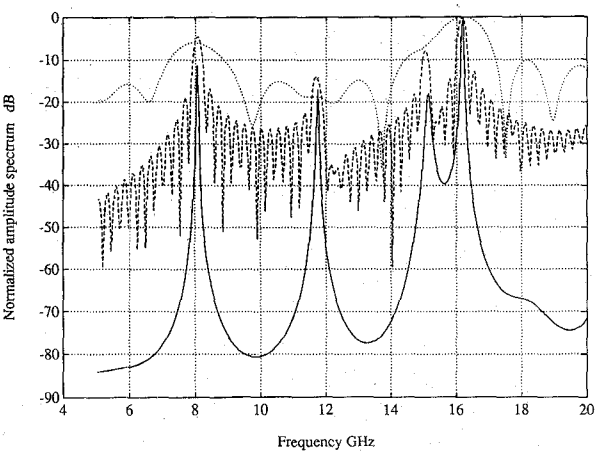

(b)

Fig. 5. Resonant frequency estimation using different methods. Dashed line: 20 000 iterations and using Fourier integration (10). Dotted line: 2000 time iterations and using Fourier integration (10). Solid line: Using 2000 time iterations in FD-TD algorithm and using digital filter processing and MUSIC method.

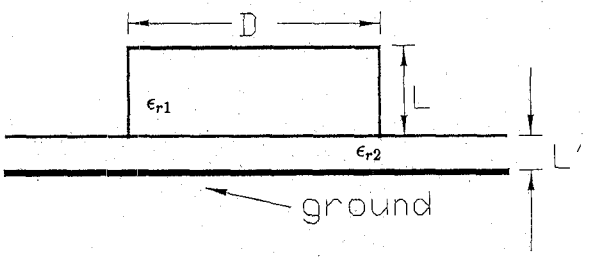

Fig. 6. Semi-open dielectric resonator on a microstrip substrate.

Dimension: $D = 11.06$ mm, $L = 4.99$ mm,
$L_1' = 1.59$ mm, $L_2' = 3.18$ mm
$\epsilon_{r1} = 35.76$, $\epsilon_{r2} = 2.2$
Dielectric region: 15 $\Delta z \times 18\ \Delta r$
$\Delta z = 0.33267$ mm, $\Delta r = 0.325294$ mm
$\Delta t = 0.65(\Delta z + \Delta r)/(2c)$, c is the speed of light in free space

The calculated and measurement results are given in Table I. In the calculation, the resonant frequencies are determined by the method presented in this paper, where

TABLE I
RESONANT FREQUENCIES FOR THE $TE_{01\delta}$ MODE OF A SEMI-OPEN DR

L' (mm)	FD-TD Results (GHz)	Measured Results (GHz)
1.59	4.9680	4.9832
3.18	4.7770	4.7918

only 2000 time iterations are used in the FD-TD calculation. For the experimental results, the DR was mounted on a substrate, and the measurements were carried out with an HP8510B network analyzer.

V. CONCLUSIONS

There are three main results coming from the present study of the FD-TD method. Digital filtering and modern spectrum estimation techniques were successfully incorporated with the FD-TD method as a means of improving its efficiency for carrying out eigenvalue analysis. The efficiency and validity of the method are demonstrated using both numerical and measured results. Another relatively new spectrum estimation method, which is called Thomson's multiple-window-method (MWM) [20], was also tested with FD-TD data. The same good frequency estimates were obtained using MWM. The second outcome of this research was the application of signal analyses to the time domain data obtained using the FD-TD algorithm. It has been shown that the FD-TD time domain signal for dielectric resonator analyses is much over sampled. The data that needs to be retained for later processing can be greatly compressed, without degrading the accuracy of the analysis. This conclusion is valid when the FD-TD method is used to analyze microstrip components and antennas. In these latter cases, the maximum frequency of time domain result, f_{max}, which sets the desampling or compressing rate, is not determined by the cutoff frequency of the FD-TD algorithm itself, but rather by the maximum frequency of the excitation gaussian pulse. According to our experience, for the analysis of microstrip antennas and components [4], [5], the data from the FD-TD results can be compressed by one order of magnitude. So, based on this conclusion, both the memory requirements for the FD-TD time domain results and the time it takes for processing the data can be reduced by at least one order of magnitude. The third result that was demonstrated by this research is that good results can be obtained by using absorbing boundary conditions when applying the FD-TD to open dielectric resonators. The validity of the analysis was demonstrated by a comparison of measurements and calculated results. All of the above conclusions are applicable to other time domain methods, such as the Transmission Line Matrix method.

In conclusion, it should be mentioned that signal processing and spectrum estimation techniques can greatly improve both the capability and the efficiency of the time domain methods. This point has been reinforced by several papers [21]–[26], where the authors have to greater or less degree drawn on signal processing techniques to improve the performance of their numerical algorithms.

ACKNOWLEDGMENT

The authors wish to thank Mr. A. Drosopoulos, Mr. C. Wu, Drs. Q. Wu, W. Chen and Mr. Y. Zhou at Communications Research Laboratory, McMaster University for their helpful discussions on this research.

REFERENCES

[1] D. Kajfez and P. Guillon, *Dielectric Resonators*. Norwood, MA: Artech House, 1986.
[2] A. Navarro, M. J. Nuñez, and E. Martin, "Study of TE_0 and TM_0 modes in dielectric resonators by a finite difference time-domain method coupled with the Discrete Fourier transform," *IEEE Trans. Microwave Theory Tech.*, vol. 39, pp. 14–17, Jan. 1991.
[3] D. H. Choi and W. J. R. Hoefer, "The finite difference-time domain method and its application to eigenvalue problems," *IEEE Trans. Microwave Theory Tech.*, vol. MTT-34, pp. 1464–1470, Dec. 1986.
[4] J. Litva, Z. Bi, K. Wu, R. Fralich, and C. Wu, "Full-wave analysis of an assortment of printed antenna structures using the FD-TD method," in *1991 IEEE AP-S Int. Symp. Dig.*, pp. 410–413, June 1991.
[5] C. Wu, K. Wu, Z. Bi, and J. Litva, "Accurate characterization of planar printed antennas using finite difference time domain method," to appear in *IEEE Trans. Antennas Propagat.*
[6] K. S. Yee, "Numerical solution of initial boundary value problems involving Maxwell's equations in isotropic media," *IEEE Trans. Antennas Propagat.*, vol. AP-14, pp. 302–307, May 1966.
[7] X. Zhang and K. K. Mei, "Time domain finite-difference approach to the calculation of the frequency dependent characteristics of microstrip discontinuities," *IEEE Trans. Microwave Theory Tech.*, vol. 36, pp. 1775–1787, Dec. 1988.
[8] J. Fang, "Time domain finite difference computation for Maxwell's equations," Ph.D. dissertation, Dept. EECS, University of California, Berkeley, 1989.
[9] G. Mur, "Absorbing boundary conditions for the finite difference approximation of the time domain electromagnetic field equations," *IEEE Trans. Electromagn. Compat.*, vol. EMC-23, pp. 377–382, Nov. 1981.
[10] C. M. Furse, S. P. Mathre, and O. P. Gandhi, "Improvements of the finite-difference time-domain method for calculating the radar cross section of a perfectly conducting target," *IEEE Trans. Microwave Theory Tech.*, vol. 38, pp.919–927, July 1990.
[11] S. Haykin, *Communication Systems*, 2nd ed. New York: Wiley, 1983.
[12] A. Taflove, "Review of the formulation and applications of the finite-difference time-domain method for numerical modeling of electromagnetic wave interactions with arbitrary structures," *Wave Motion 10*, pp. 547–582, 1988.
[13] A. Taflove and K. R. Umashankar, "Advanced numerical modeling of microwave penetration and coupling for complex structures," Final Report No. UCRL-15960, Contract 6599805, Lawrence Livermore Nat. Lab., 1987.
[14] D. F. Elliott, Handbook of digital signal processing, engineering applications, New York: Academic, 1987.
[15] J. N. Little, "Signal processing toolbox for use with Matlab," *The Math Works, Inc.*, 1988.
[16] P. Stoica and T. Söderström, "Statistical analysis of MUSIC and subspace rotation estimates of sinusoidal frequencies," *IEEE Trans. Acoust., Speech, Signal Processing*, vol. 39, pp. 1836–1847, Aug. 1991.
[17] S. Haykin, *Adaptive Filter Theory*, 2nd ed. Englewood Cliffs, NJ: Prentice-Hall, 1991.
[18] S. L. Marple, Jr., *Digital Spectrum Analysis with Applications*. Englewood Cliffs, NJ: Prentice-Hall, 1987.
[19] P. Stoica and T. Söderström, "On spectral and root forms of sinusoidal frequency estimators,"in *Proc. IEEE Int. Conf. Acoust., Speech, Signal Processing, ICASSP'91*, Toronto, Canada, pp. 3257–3260.
[20] A. Drosopoulos and S. Haykin, "Adaptive radar parameter estima-

tion with Thomson's Multiple-Window method," ch. 7, in S. Haykin and A. Steinhardt Eds., *Adaptive Radar Detection and Estimation*. New York: Wiley, 1991.

[21] Z. Bi, K. Wu, C. Wu, and J. Litva, "A Dispersive boundary condition for microstrip component analysis using the FD-TD method," *IEEE Trans. Microwave Theory Tech.*, vol. 40, no. 4, pp. 774–777, Apr. 1992.

[22] J. G. Blaschak and T. G. Moore, "Adaptive absorbing boundary condition," presented at *Progress in Electromagnetics Research Symp.*, Cambridge, MA, July 1991.

[23] W. L. Ko and R. Mittra, "A combination of FD-TD and prony's method for analyzing microwave integrated circuits," in *IEEE AP-S Int. Symp. Dig.*, June 1991, pp. 1742–1745.

[24] S. T. Chu and S. K. Chaudhuri, "Combining modal analysis and the FD-TD method in the study of dielectric waveguide problems," *IEEE Trans. Microwave Theory Tech.*, vol. 38, pp. 1755–1760, Nov. 1990.

[25] Z. Bi, J. Litva, K. Wu, and C. Wu, "Using digital signal processing techniques with the FD-TD method, " presented at 1992 IEEE-APS/URSI/NEM Joint Symposia, Chicago, July 1992.

[26] Z. Bi, K. Wu and J. Litva, "Designing dispersive boundary condition (DBC) for the FD-TD method using digital filtering theory," in 1992 AP-S Int. Symp. Dig., July 1992.

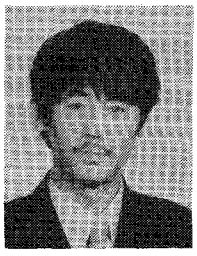

Zhiqiang Bi (S'91) was born in Shandong, China, on March 15, 1961. He received the B.S. and M.S.E. degrees from Dalian Maritime University, Dalian, China, in 1982 and 1986, respectively.

He was a Research Assistant from 1982 to 1983, a Teaching Assistant from 1986 to 1988, and a Lecturer from 1988 to 1989 in Dalian Maritime University, where he was teaching and doing research in digital signal processing and detection and estimation theories and techniques. Since 1989, he has been a Teaching Assistant in the Department of Electrical and Computer Engineering at McMaster University, Hamilton, ON, Canada, where he is working toward the Ph.D. degree. His current research interests include propagation and scattering of electromagnetic waves, design of microwave devices by using numerical and analytical methods, and digital signal processing.

Ying Shen was born in Shanghai, China, on June 10, 1962. He received the B.S. and M.S. degrees from Shanghai University of Science and Technology, Shanghai, China, in 1984 and 1987, respectively.

From 1987 to 1988, he was a Teaching Assistant, and from 1988 to 1990 a Lecturer in the Radio-Electronics Department of Shanghai University of Science and Technology, Shanghai. Since 1991, he has been a Teaching Assistant in the Department of Electrical and Computer Engineering at McMaster University, where he is working toward the Ph.D. degree. His current research interests include the desigh of microwave monolithic integrated circuits, integrated active antennas and FDTD method for analyzing microwave components.

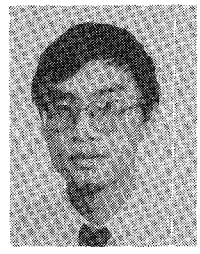

Ke-Li Wu (M'90) was born in Hubei, China, on November 1, 1959. He received the B.S. and M.S.E. degrees from the East China Institute of Technology, Nanjing, China, in 1982 and 1985, respectively, and the Ph.D. degree from Laval University, Quebec, Canada, in 1989, all in electrical engineering.

He was a Research Assistant in the East China Institute of Technology, from 1985 to 1986. From 1989 to 1990 he was a Postdoctorate Fellow at McMaster University, Hamilton, ON, Canada. He joined the Integrated Antenna Group, Communications Research Laboratory, McMaster University, Canada, in 1990 as Research Engineer. In 1991 he also became an Assistant Professor (part-time) of Electrical and Computer Engineering at McMaster University. His professional interests include all aspects of numerical methods in electromagnetics with emphasis on integrated antennas, microwave circuits, electromagnetic scattering and integrated circuit packaging.

Dr. Wu contributed to *Finite Element and Finite Difference Methods in Electromagnetic Scattering*, Volume 2 of *Progress in Electromagnetics Research* (Elsevier, 1990) and to *Computational Electromagnetics* (North-Holland, 1991).

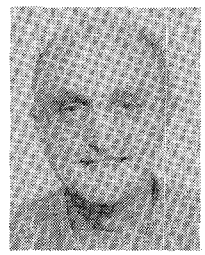

John Litva (M'82) is currently a Professor in Electrical Engineering at McMaster University, Hamilton, Ontario, Canada, and is the holder of the Microwave Antenna Chair sponsored by Spar Aerospace and Andrew Canada. As well, he is a Thrust Leader in the Telecommunications Research Institute of Ontario (TRIO). TRIO is a university-industry based Centre of Excellence, which is funded by the Province of Ontario, and whose mandate is to conduct research in support of the telecommunications industry in Ontario. Prior to 1985 he was a Research Scientist in the Radar Laboratory at the Communications Research Centre in Ottawa, where his primary area of research was low-angle radar tracking of sea skimming missiles. At present his research interests are centered on 1) low-angle radar tracking (matched field processing), 2) scattering theory, 3) radio-wave direction finding, and 4) phased-array antenna theory.